Thermochimica Acta 502 (2010) 20–23

Contents lists available at ScienceDirect

Thermochimica Acta

journal homepage: www.elsevier.com/locate/tca

The use of Differential Scanning Calorimetry (DSC) to characterize phase diagrams of ionic mixtures of 1-n-butyl-3-methylimidazolium chloride and niobium chloride or zinc chloride

Melquizedeque B. Alves [a], Alexandre P. Umpierre [a], Vianney O. Santos Jr. [a], Valerio C.D. Soares [a], Jairton Dupont [b], Joel C. Rubim [a], Paulo A.Z. Suarez [a,*]

[a] *Laboratório de Materiais e Combustíveis - Instituto de Química da Universidade de Brasília, C.P. 04478, CEP 70904-970, Brasília, DF, Brazil*
[b] *Laboratório de Catálise Molecular - Instituto de Química da Universidade Federal do Rio Grande do Sul, C.P. 15003, CEP 91501-970, Porto Alegre, RS, Brazil*

ARTICLE INFO

Article history:
Received 23 September 2008
Received in revised form 15 January 2010
Accepted 23 January 2010
Available online 2 February 2010

Keywords:
DSC
Phase diagram
Ionic liquids
Niobium pentachloride
Zinc chloride
1-n-butyl-3-methylimidazolium

ABSTRACT

The thermal behavior of the BMICl/$NbCl_5$ and BMICl/$ZnCl_2$ mixtures was investigated by DSC and correlated with previous studies using Raman spectroscopy. Combining both results, it was possible to built the phase diagram for these mixtures and suggest the formation of different compounds and the equilibria in the euthetic mixtures. The phase diagram of BMICl and $NbCl_5$ mixture showed that probably only one compound is formed at $X_{NbCl5} = 0.50$ ($BMINbCl_6$) and euthetic mixtures are present in the $0 \leq X_{NbCl5} \leq 0.50$ composition range. For the BMICl and $ZnCl_2$, four different compounds were detected: $(BMI)_2(ZnCl_4)$ for $X_{ZnCl2} = 0.35$; $(BMI)_2(Zn_2Cl_6)$; $(BMI)_2(Zn_3Cl_8)$ and $(BMI)_2(Zn_4Cl_{10})$ for $X_{ZnCl2} = 0.70$, and between these isoplets euthetic mixtures are formed.

1. Introduction

Molten salts or ionic liquids (ILs), in particular those derived from ionic salts of the 1,3-dialkylimidazolium cation have received considerable attention as an alternative class of solvents [1]. By changing the alkyl substituents and/or the anions it is possible to tune their physical–chemical properties according to the desired use [2,3].

Among the ILs derived from 1,3-dialkylimidazolium cation one important class is that obtained by the mixture of their halide salts and transition-metal halides, such as 1-n-butyl-3-methylimidazolium chloride (BMICl) mixed with $AlCl_3$ [4], $FeCl_3$ [5,6], $ZnCl_2$ [7,8], $InCl_3$ [9], $PdCl_2$ [10,11]. Some of them have been successfully used as the “mobile phase” for the biphasic transition-metal catalyzed reactions [4,10,11] or as immobilizing agents in organometallic catalysis [7]. Another application for such kind of ILs relies on the fact that the presence of a transition metal can promote Lewis acid catalytic processes [4,8,9,12]. With no doubt, the ILs derived from mixtures of 1,3-dialkylimidazolium chlorides and $AlCl_3$ are the most investigated ones [4]. Due to the acceptor/donor patterns, these ionic liquids present Lewis properties also dependent on the amount of the aluminum halide. It is worth mentioning that the Lewis acidity can be expressed in terms of the molar fraction of the aluminum compound (X), being called acidic the mixtures with $X > 0.5$ (or 50 mol%), basic when $X < 0.5$ and neutral when $X = 0.5$. Despite the inconvenience of the great reactivity of theses compounds towards air and water, their Lewis acidity makes them especially useful in Ziegler–Natta type catalytic systems and acid catalyzed organic reactions, e.g. olefin dimerization, alkylation, Friedel–Crafts, Diels–Alder, and Pechmann reactions [13–18].

ILs derived from 1,3-dialkylimidazolium chlorides and $AlCl_3$ were also investigated regarding to their structure [4,19]. Depending on the molar proportions of $AlCl_3$ and the other chloride salts added to the mixture, the formation of $AlCl_4^-$, $Al_2Cl_7^-$, and $Al_3Cl_{10}^-$ anionic species were identified [4,20]. The composition of the mixtures of alkylimidazolium chlorides and other transition-metal chlorides as $FeCl_3$ and $FeCl_2$ [5,6] $ZnCl_2$ [20], $AuCl_3$ [21], $InCl_3$ [22] has also been investigated.

We and others have demonstrated the technological potential of these binary mixtures. For example the ILs obtained by the mixture of BMICl and $NbCl_5$ act as catalysts for the synthesis of coumarins by the Pechmann reaction [12], and the mixture of BMICl and $ZnCl_2$ can be used as reactional system for olefin and aromatic compounds hydrogenation [7].

In binary mixtures that can react and produce new compounds, the number of constituents of the mixture is greater than that of

---

* Corresponding author. Tel.: +55 61 33072167; fax: +55 61 32734149.
E-mail address: psuarez@unb.br (P.A.Z. Suarez).

0040-6031/$ – see front matter © 2010 Elsevier B.V. All rights reserved.
doi:10.1016/j.tca.2010.01.023

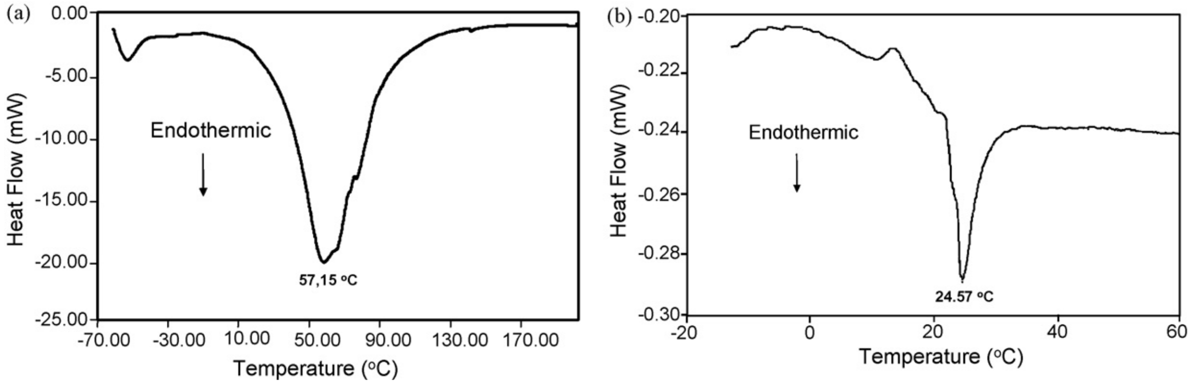

Fig. 1. Illustrative selected thermograms obtained for BMICl/$NbCl_5$, $X_{NbCl5} = 0.50$, (a) and BMICl/$ZnCl_2$, $X_{ZnCl2} = 0.22$, (b) ionic mixtures.

the two starting components, and, therefore, the phase diagram may also present several euthetic points. The main reason for this is that the system can show phase transition temperatures lower than their components, enabling the identification of euthetic points. In the case of liquid and solid phase diagrams, a solid with eutectic composition melts, without change in composition, in a temperature lower than the melting temperature of any other mixture.

In a previous work we have used Raman spectroscopy to identify the anionic species formed in mixtures of 1-n-butyl-3-methylimidazolium chloride with different amounts of niobium pentachloride ($NbCl_5$) or zinc dichloride ($ZnCl_2$) [23]. In this work we aimed the used of Differential Scanning Calorimetry (DSC) to determine the phase diagrams for these mixtures. Therefore, the strategy to investigate the ionic species present in these mixtures as well as the interaction of anions and cations will be done through the DSC and vibrational (Raman) analysis of mixtures of different molar ratios of BMICl and $NbCl_5$ or $ZnCl_2$. In both cases, the correct identification of the anionic species, that act as Lewis acids, is fundamental for the understanding of the catalytic process they take part.

2. Experimental

2.1. General

All manipulations were performed under dry, oxygen-free argon using standard Schlenk tube techniques. All solvents were dried over suitable desiccant agents and distilled under argon prior to use. Differential Scanning Calorimetry measurements of BMICl/$NbCl_5$ mixtures were performed in a Shimadzu DSC-50 under helium flow and of BMICl/$ZnCl_2$ mixtures were performed in a TA 1200-PL-DSC under nitrogen flow. 10.0 mg samples were placed in aluminum pans sealed and cooled with liquid nitrogen down to −70 °C, then the samples were heated at 10 °C min^{-1} of heating rate up to 200 °C. The experimental details with regard to the Raman measurements can be found in ref. [23].

2.2. Materials

The BMICl was prepared according to literature procedures [24] and commercial $ZnCl_2$ was dried by benzene azeotropic distillation and stored under nitrogen. All other chemical were obtained from commercial sources (Aldrich) and used as received. Commercial niobium pentachloride obtained from CBMM (Companhia Brasileira de Metalurgia e Mineração) was distilled under vacuum and stored under nitrogen atmosphere. The estimated purities of BMICl, $ZnCl_2$ and $NbCl_5$ are up to 98%.

The BMICl/$ZnCl_2$ mixtures were prepared by mixing appropriate amounts of solid BMICl and $ZnCl_2$ over nitrogen and an efficient stirring at 70 °C forming pale-yellow viscous ionic liquids which becomes homogeneous easily.

The preparation of the organo-niobate ILs was carried out by mixing BMICl and $NbCl_5$ at different mol ratios using standard Schlenk technique. The desired amounts of BMICl and $NbCl_5$ were placed in a Schlenk tube and kept under magnetic stirring at 70 °C until complete homogenization was obtained. The 50% mixture yields pale brown solids at room temperature, which become browned-red viscous ILs when melted.

3. Results and discussion

The DSC study for the different ionic mixtures showed a large range in phase-transition temperatures according to the $NbCl_5$ or $ZnCl_2$ content in the mixtures. It has been observed that the BMICl/$ZnCl_2$ mixtures are liquid at room temperature and they were very difficult to be crystallized. Therefore, a low cooling rate (−1 °C min^{-1}) was needed in order to see the thermal events. Illustrative selected thermograms obtained for BMICl/$NbCl_5$, $X_{NbCl5} = 0.50$, (a) and BMICl/$ZnCl_2$, $X_{ZnCl2} = 0.22$, (b) ionic mixtures are shown in Fig. 1.

3.1. BMICl/$NbCl_5$ ionic mixtures

The ionic mixtures of BMICl and $NbCl_5$ were prepared in the following molar fractions $X = 0.1$, 0.2, 0.3, 0.4, 0.5, 0.6 and 0.7 (X = the content of $NbCl_5$ in molar fraction in the $NbCl_5$/BMICl mixture). It is worth mentioning that $NbCl_5$ does not exist at room temperature, i.e., it is added as the dimer, Nb_2Cl_{10} [23]. The phase transition temperatures for the different mixtures are presented in Fig. 2, as obtained from DSC measurements. At $X_{NbCl5} = 0$, the

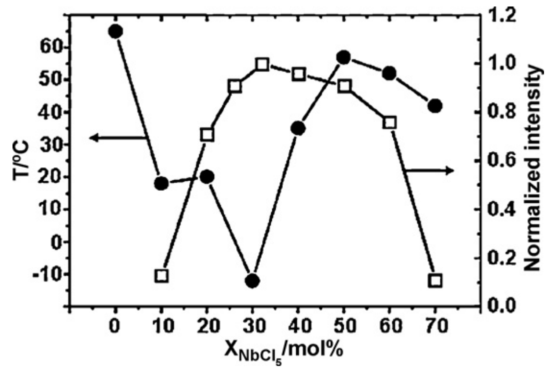

Fig. 2. (●) Phase transition temperature of BMICl/$NbCl_5$ mixtures and (□) normalized Raman intensity of the $NbCl_6^-$ symmetric stretching mode (371 cm^{-1}) as a function of the mole fraction of $NbCl_5$.

melting temperature is that of pure BMICl. As the amount of $NbCl_5$ increases the melting point of the mixture diminishes, affording a minimum for $X_{NbCl5} = 0.3$. With higher amounts of $NbCl_5$, the melting point increases up to 57 °C for $X_{NbCl5} = 0.5$ and starts again to decrease. The Raman spectroscopic investigation of these mixtures have shown that the anion $NbCl_6^-$ is present in all compositions of BMICl/$NbCl_5$ mixtures and is the only niobium specie detected bellow $X_{NbCl5} < 0.50$ [23]. For $X_{NbCl5} > 0.50$ the neutral Nb_2Cl_{10} specie is also observed mixed with $NbCl_6^-$. Probably the isoplet in the phase diagram near $X_{NbCl5} = 0.5$ corresponding to the (BMI)($NbCl_6$) IL formed. We can then conclude that for compositions from $X_{NbCl5} = 0$ to $X_{NbCl5} = 0.5$, the species (BMI)($NbCl_6$) and BMICl are present. For $X_{NbCl5} = 0.5$ or higher, probably the only species present are (BMI)($NbCl_6$) and Nb_2Cl_{10}. To illustrate the correlation between the phase diagram and the Raman results, Fig. 2 also shows the dependence of the Raman intensity (normalized) of the 371 cm^{-1} symmetric stretching mode of $NbCl_6^-$ [23] as a function of the $NbCl_5$ molar fraction. It is worth mentioning that the Raman investigation of this system showed no evidence for the formation of any different anionic specie for compositions corresponding to $X_{NbCl5} < 0.50$. Therefore, the discontinuity observed in the phase diagram of Fig. 2 for $X_{NbCl5} < 0.50$ has no real significance and is probably due to some impurity or other experimental problem. Nonetheless, Raman spectroscopy and the phase diagram obtained by DSC analysis seems to be in good agreement and strong suggesting that there is a euthetic behavior for mixtures of BMICl and $NbCl_5$ with compositions $0 \leq X_{NbCl5} \leq 0.50$. It is worth mentioning that although the Raman spectroscopy showed only one ionic species for mixtures with $X_{NbCl5} \leq 0.50$ it is possible to observe a discontinuity in the diagram obtained using DSC data. We believe this has no real significance and is probably due to impurities produced after the decomposition of the high Lewis acid $NbCl_5$, which decomposes in the presence of moisture even in low amounts.

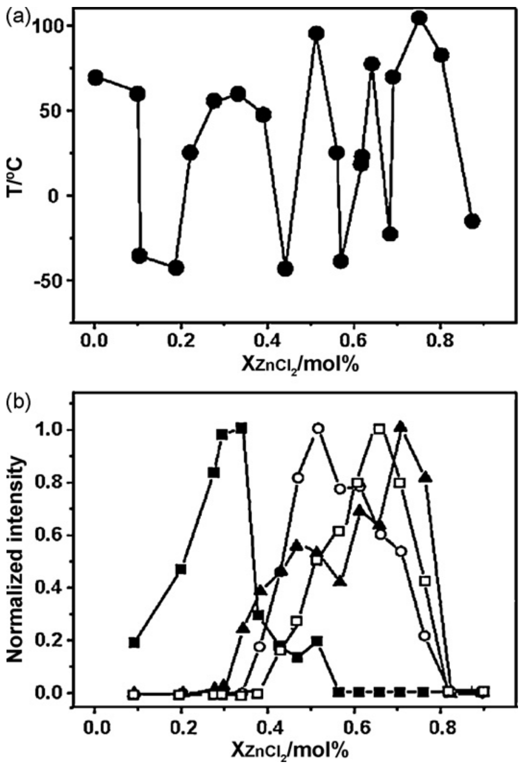

Fig. 3. (a) Phase transition temperatures for the BMICl/$ZnCl_2$ mixtures and (b) normalized Raman intensities as a function mole fraction of $ZnCl_2$. (■) = 276 cm^{-1}, $ZnCl_4^{2-}$; (○) = 317 cm^{-1}, $Zn_2Cl_6^{2-}$; (□) = 265 cm^{-1}, $Zn_3Cl_8^{2-}$; (▲) = 340 cm^{-1}, $Zn_4Cl_{10}^{2-}$.

3.2. The BMI/$ZnCl_2$ ionic mixtures

Following the same methodology described above several mixtures of BMICl and $ZnCl_2$ were prepared and their respective melting temperatures were obtained by DSC. These data were used to draw a phase diagram that is displayed in Fig. 3(a). As can be depicted from this figure, the behavior of BMICl/$ZnCl_2$ mixtures are much more complex than those observed for BMICl/$NbCl_5$ ones. Indeed, this plot shows up to four points of temperature minima, probably each one corresponding to euthetic points ($X_{ZnCl2} = 0.15$, −42 °C; $X_{ZnCl2} = 0.43$, −42 °C; $X_{ZnCl2} = 0.58$, −40 °C; $X_{ZnCl2} = 0.68$, −25 °C). It is also possible to clearly identify the four isoplets that pass through the points of maximum ($X_{ZnCl2} = 0.33$, 60 °C; $X_{ZnCl2} = 0.50$, 100 °C; $X_{ZnCl2} = 0.65$, 92 °C; $X_{ZnCl2} = 0.75$, 110 °C).

The Raman spectra of BMICl/$ZnCl_2$ mixtures were already investigated and different anionic species were characterized according to the mixture composition [23]. For comparison purposes, Fig. 3(b) shows the dependence of the normalized Raman intensities of vibrational modes characteristic of four different $[Zn_xCl_{2x+2}]^{2-}$, $x = 1–4$ (see ref. [23] for a detailed discussion on the vibrational assignment). Note that the maxima observed in the Raman intensities correlate very well with the four isoplets depicted in Fig. 3(a). In this sense, predominant anionic species are $ZnCl_4^{2-}$ for $X_{ZnCl2} = 0.35$; $Zn_2Cl_6^{2-}$ for $X_{ZnCl2} = 0.50$; $Zn_3Cl_8^{2-}$ for $X_{ZnCl2} = 0.64$ and $Zn_4Cl_{10}^{2-}$ for $X_{ZnCl2} = 0.70$, suggesting the formation of the compounds $(BMI)_2(ZnCl_4)$, $(BMI)_2(Zn_2Cl_6)$, $(BMI)_2(Zn_3Cl_8)$, and $(BMI)_2(Zn_4Cl_{10})$. Thus, as in the previous case for the mixtures of BMICl and $NbCl_5$, the Raman results are in perfect agreement to those obtained by the DSC analysis of BMICl and $ZnCl_2$ mixtures. These results also show that between those isoplets it is possible to identify the binary euthetic mixtures: BMICl and $(BMI)_2(ZnCl_4)$ for $0 \leq X_{ZnCl2} \leq 0.35$; $(BMI)_2(ZnCl_4)$ and $(BMI)_2(Zn_2Cl_6)$ for $0.35 \leq X_{ZnCl2} \leq 0.50$; $(BMI)_2(Zn_2Cl_6)$ and $(BMI)_2(Zn_3Cl_8)$ for $0.50 \leq X_{ZnCl2} \leq 0.64$; $(BMI)_2(Zn_3Cl_8)$ and $(BMI)_2(Zn_4Cl_{10})$ for $0.64 \leq X_{ZnCl2} \leq 0.70$; and $(BMI)_2(Zn_4Cl_{10})$ for $X_{ZnCl2} \geq 0.70$. It is important to highlight that similar dialquil-imidazolium zinc halides have already been prepared using for $X_{ZnX2} = 0.50$ [25] and that the molecular structure determined by single crystal X-ray diffraction analysis confirmed the formation of the complex (1,3-dimethylimidazolium)$_2$($ZnBr_2Cl_2$), which is close to the compound observed here for $0.50 \geq X_{ZnCl2}$ (see Fig. 3).

4. Conclusions

In summary, with the use of DSC analysis and Raman spectroscopy of mixtures of BMICl and $NbCl_5$ or BMICl and $ZnCl_2$, it was possible to describe their phase diagrams. Five different isoplets corresponding to the formation of (BMI)($NbCl_6$), $(BMI)_2(ZnCl_4)$, $(BMI)_2(Zn_2Cl_6)$, $(BMI)_2(Zn_3Cl_8)$ and $(BMI)_2(Zn_4Cl_{10})$ salts and five euthetic mixtures with different Lewis acidic anions. These results are particularly important in organic synthesis because they can be used to describe these mixtures and understand the acidic catalytic processes they take place as well as to design ionic mixtures with desired anionic species, and, thus, tuning the acidity of the media.

Acknowledgments

The authors thank FINATEC, FINEP-CTPETRO, CNPq-CTPETRO, CNPq-UNIVERSAL, and CAPES for financial support and CNPq for research fellowships.

Appendix A. Supplementary data

Supplementary data associated with this article can be found, in the online version, at doi:10.1016/j.tca.2010.01.023.

References

[1] J. Dupont, R.F. de Souza, P.A.Z. Suarez, Chem. Rev. 102 (2002) 3667–3691.
[2] P.A.Z. Suarez, C.S. Consorti, R.F. de Souza, J. Dupont, Quim. Nova 24 (2001) 830–837.
[3] H. Weingartner, Angew. Chem. Int. Ed. 47 (2008) 654–670.
[4] T. Welton, Chem. Rev. 99 (1999) 2071–2083.
[5] M.S. Sitze, E.R. Schreiter, E.V. Patterson, R.G. Freeman, Inorg. Chem. 40 (2001) 2298–2304.
[6] P. Koelle, R. Dronskowski, Inorg. Chem. 43 (2004) 2803–2809.
[7] J. Dupont, P.A.Z. Suarez, A.P. Umpierre, R.F. de Souza, Catal. Lett. 73 (2001) 211–213.
[8] C. Vallee, C. Valerio, Y. Chauvin, G.P. Niccolai, J.-M. Basset, C.C. Santini, J.-C. Galland, B. Didillon, J. Mol. Catal. A 214 (2004) 71–81.
[9] B.A. da, S. Neto, G. Ebeling, R.S. Gonçalves, F.C. Gozzo, M.N. Eberlin, J. Dupont, Synthesis (2004) 1155–1158.
[10] J.E.L. Dullius, P.A.Z. Suarez, S. Einloft, R.F. de Souza, J. Dupont, J. Fischer, A. De Cian, Organometallics 17 (1988) 815–819.
[11] S.M. Silva, P.A.Z. Suarez, R.F. de Souza, J. Dupont, Polym. Bull. 40 (1998) 401–405.
[12] V.C.D. Soares, M.B. Alves, E.R. Souza, I.O. Pinto, J.C. Rubim, C.K.Z. Andrade, P.A.Z. Suarez, Int. J. Mol. Sci. 8 (2007) 392–398.
[13] Y. Chauvin, S. Einloft, H. Olivier, Ind. Eng. Chem. Res. 34 (1995) 1149–1155.
[14] S. Einloft, F.K. Dietrich, R.F. de Souza, J. Dupont, Polyhedron 19 (1996) 3257–3259.
[15] M.H. Valkenberg, C. de Castro, W.F. Hölderich, Appl. Catal. A 215 (2001) 185–190.
[16] T. Fischer, A. Sethi, T. Welton, J. Woolf, Tetrahedron Lett. 40 (1999) 793–796.
[17] M.K. Potdar, S.S. Mohile, M.M. Salunkhe, Tetrahedron Lett. 42 (2001) 9285–9287.
[18] A.C. Khandekar, B.M. Khadilkar, Synlett 1 (2002) 152–154.
[19] T.A. Zawodzinski, R.A. Osteryoung, Inorg. Chem. 28 (1989) 1710–1715.
[20] V. Lecocq, A. Graille, C.C. Santini, A. Baudouin, Y. Chauvin, J.M. Basset, L. Arzel, D. Bouchu, B. Fenet, New J. Chem. 29 (2005) 700–706.
[21] M. Hasan, I.V. Kozhevnikov, M. Siddiqui, H. Rafiq, A. Steiner, N. Winterton, Inorg. Chem. 38 (1999) 5637–5641.
[22] J.-Z. Yang, P. Tian, W.-G. Xu, B. Xu, S.-Z. Liu, Thermochim. Acta 412 (2004) 1–5.
[23] M.B. Alves, V.O. Santos Jr., V.C.D. Soares, P.A.Z. Suarez, J.C. Rubim, J. Raman Spectrosc. 39 (2008) 1388–1395.
[24] P.A.Z. Suarez, J.E.L. Dullius, S. Einloft, R.F. de Souza, J. Dupont, Polyhedron 15 (1996) 1217–1219.
[25] J. Palgunadi, O.S. Kwon, H. Lee, J.Y. Bae, B.S. Ahn, N.Y. Min, H.S. Kim, Catal. Today 98 (2004) 511–514.